Computers and Concrete, Vol. 7, No. 2 (2010) 119-143

DOI: http://dx.doi.org/10.12989/cac.2010.7.2.119

The use of RKPM meshfree methods to compute responses to projectile impacts and blasts nearby charges

Hyung-Jin Choi*, John Crawford and Youcai Wu

Karagozian & Case, 2550 N. Hollywood Way, Suite 500, Burbank, CA 91505, USA

(Received November 11, 2009, Accepted November 30, 2009)

Abstract. This paper presents results from a study concerning the capability afforded by the RKPM (reproducing kernel particle method) meshfree analysis formulation to predict responses of concrete and UHPC components resulting from projectile impacts and blasts from nearby charges. In this paper, the basic features offered by the RKPM method are described, especially as they are implemented in the analysis code KC-FEMFRE, which was developed by Karagozian & Case (K&C).

Keywords: ultra high performance concrete; meshfree method; reproductive kernel particle method; penetration; crater analysis.

1. Introduction

The motivation for the work described in this paper is related to the need to enhance the current technology for analyzing the interaction between concrete and reinforced concrete structural components and such severe load scenarios as those associated with projectile impacts and blasts from nearby detonations. For a decade or so, a new family of methods, collectively called meshfree methods, which seem to offer great promise for the analysis of problems that exhibit these kinds of severe response and damage states, has attracted interest. This paper describes one of these meshfree methods and its implementation in an analysis codes, and shows some initial response predictions to demonstrate the ability afforded to predict response of concrete component's subjected to severe loadings.

Meshfree methods seem inherently more able to effectively address impact and intense blast kinds of analysis problems, which seem to present a struggle for older methods, such as the finite element method that employ a mesh as a means to discretize the problem. Meshfree methods hold particular promise for addressing the complex physics problems associated with fragment and projectile penetrations and contact detonations (i.e., FPP/CD problems). Moreover, the potential capability offered by the meshfree formulation is thought to be paramount to obtaining the needed improvements in analysis results. The intent in this paper is to describe an enhanced set of numerical methods for modeling effects on structural components related to FPP/CD problems.

Meshfree methods do not use a mesh to discretize the domain of the structural systems to be analyzed. Instead, the domain to be analyzed is discretized by a set of particles (sometimes called nodes), where the shape functions associated with each particle exhibit a compact support (i.e.,

* Corresponding author, Ph.D., E-mail: choi@kcse.com

cover a small portion of the whole domain), which includes a few neighbor particles. Using the meshfree formulation, an approximation of the system's behavior can be constructed for computing field variables (e.g., displacements and velocities) and state variables (e.g., stress and strain) for the domain as a whole without the need for a mesh. The family of meshfree methods (MFM) incorporates the main advantages of the finite element method (FEM), by likewise providing compact supports for its shape functions with good approximation properties, while avoiding the main disadvantages of the finite element method caused by excessive mesh distortion and the need for ad hoc methods to stabilize the calculation, such as erosion and hourglass control that often introduce a good deal of uncertainty into an analysis.

1.1. KC-FEMFRE code

Of particular interest in developing an analysis code was the creation of a code that combines the best features of FEM and meshfree formulations. As a result, the meshfree analysis code KC-FEMFRE (Choi *et al.* 2009) was developed. This code was developed by Karagozian & Case (K&C), to provide a working MFM/FEM code that was particularly suited to solving FPP/CD problem, and as such several novel features were incorporated into it that are thought to be singularly useful in addressing these kinds of problems. The code offers sufficient capability and capacity to perform calculations suitable for assessing the effectiveness of the coupled MFM/FEM techniques for tackling FPP/CD problems and affords a means for demonstrating the potential benefits that can be gleaned from this form of analytic approach.

The paper briefly describes the features of the KC-FEMFRE code, some aspects of its development, and examples of the code's application. The effort in creating the KC-FEMFRE code built on past K&C efforts (Chen and Crawford, 2005, 2006), where K&C teamed with UCLA (University of California at Los Angeles), to develop the theoretical basis needed to deliver a working meshfree code that can analyze realistic FPP/CD problems.

In developing KC-FEMFRE, a broad-based analytic capability was envisioned that was focused on those aspects of FPP/CD problems that are not well addressed with present simulation software (e.g., codes such as LS-DYNA (LS-DYNA 2007)). As a result, this code offers an array of new techniques involving the meshfree formulation; some of these are highlighted in Table 1. The most important of these features is the ability to deploy coupled MFM/FEM models that offer an evolutionary coupling, whereby the conventional FEM formulation is used to span the whole domain of the problem at the outset and is only replaced locally with a meshfree formulation if the FEM formulation breaks down.

In K & C's approach, the Reproducing Kernel Particle Method (RKPM) meshfree formulation, which was introduced by (Chen *et al.* 1996, 1997, 1998, Chen and Wang 2000, Chen *et al.* 1998), was selected as the meshfree method to be used. RKPM was chosen because it seems most suitable to providing the coupled FEM/MFM modeling capability desired.

1.2. Studies presented

This paper presents results from several studies concerning the capability afforded by the KC-FEMFRE code and in particular by the RKPM analysis formulation to predict responses of concrete and ultra-high performance concrete (UHPC) components resulting from projectile impacts and blasts from nearby charges.

Table 1 Key features of the KC-FEMFRE code

Type of Feature	Purpose
1. RKPM formulation	This feature provides a standalone modeling capability using an MFM formulation that is based on the reproducing kernel particle method (RKPM). The RKPM offers an MFM formulation that is easily integrated with the LFEM formulation, through in contrast to LFEM, the RKPM shape functions overlap one another (Fig. 1).
2. Lagrangian FEM formulation	This feature provides a standalone standard Lagrangian FEM approach (LFEM) to modeling with 8-node solid elements. The only difference between this approach and standard LFEM formulation is that the state variables are carried at the nodal points. This facilitates the transition process (i.e., in evolutionary coupling, Feature 4) employed in converting an LFEM domain to an RKPM domain.
3. LFEM-RKPM Coupling Techniques	This feature allows models to be constructed having both LFEM and RKPM regions. Coupling functions were constructed by imposing reproducing conditions of the combined LFEM and RKPM shape functions and by introducing a ramp function to achieve the coupling of the LFEM and RKPM approximations (see Fig. 2). This coupling transpires over a finite transition zone where the combined influence of the LFEM and RKPM shape functions are considered. This has provided a versatile and effective means to connect LFEM and RKPM discretizations.
4. Automated Evolutionary Coupling of LFEM and RKPM Domains	This feature provides an evolutionary coupling capability for converting the discretization from an LFEM domain to an RKPM domain, thus allowing replacement of the portions of the LFEM domain that are numerically unsound. This feature employs a triggering device that indicates where and when the updating/evolution is to occur and to what extent. Because state and field variables are held at the node points in both the LFEM/RKPM formulations and the same material models are used for both, the conversion process is a relatively straightforward task.
5. Stabilized Nodal Integration	Nodal integration methods, which are a standard means for integrating in Spherical Particle Hydrodynamics (SPH) codes, tend to produce oscillations in computed displacement fields for small support sizes. To address this concern, new stabilized nodal integration procedures for RKPM were developed. These methods are also used for the LFEM domain. These include (Fig. 3): SCNI: Stabilized conforming nodal integration. SNNI: Stabilized non-conforming nodal integration, for large deformations. SD-NI: Subdomain nodal integration using SCNI for the Lagrangian domains and SNNI for the semi-Lagrangian domains.
6. Semi-Lagrangian Formulation	Large strain gradients, large deformations, distortions, and fractures are anticipated for FPP/CD problems. To accommodate these without excessively distorting the kernel support of a specific particle, a semi-Lagrangian approach is adopted. Here the kernel support is allowed to deform independently of the material deformation (Fig. 4). This means that the mass conservation inherent within the kernel, which is implied by the Lagrangian formulation, is lost and that a correction is needed to account for the loss/gain of mass within a specific kernel.
7. Contact Algorithms	Natural kernel contact algorithms were developed to effectuate modeling of multi-body contact of flexible bodies and self-contact between material particles.
8. Adaptive Fidelity RKPM Discretization	This feature is related to increasing/decreasing the fidelity of the discretization in regions of the meshfree domain. The adaptive fidelity of the RKPM discretization is automated, which is based on some form of criteria or triggering device to initiate the process and govern the extent of the change in fidelity.
9. Material Models	Four types of material models are provided by KC-FEMFRE, which can be used by either the LFEM or RKPM formulation. These are the K&C concrete model (Albertsen 1973), piecewise linear von Mises model with fracture, a cap model, and an elastic model.

In these studies, results from KC-FEMFRE are compared to test results and results computed by LS-DYNA to demonstrate the capabilities afforded and to indicate the compatibility of the KC-FEMFRE results with behaviors observed in tests and provided by the conventional Lagrangian FEM formulation. The objectives of the studies presented herein include:

- Assessing the differences between RKPM and LFEM results.
- Achieving a better understanding of the influence of modeling choices on the magnitude and form of predicted response and damage for FPP/CD problems.
- Comparing of behaviors engendered by fragment impacts to those caused by contact charges and similar forms of intense pressure pulses.

It is important to evaluate these influences for two key reasons:

- The obvious: to do better analyses
- But of equal importance is to better understand the consequences of the compromises that often need to be made for the sake of practicality (i.e., assessing the level of error introduced in the response by the use of less than ideal models). For example, it is often impractical to use the very dense discretizations that are needed in the analyses of actual structural components and systems to capture the types of responses and loadings generated by high velocity fragment impacts and contact charges.

Next some of the features of the KC-FEMFRE code are described. After that, several examples of its use are shown to illustrate some of the codes capabilities. Most of the results shown are computed using either (1) the Lagrangian finite element method (LFEM), as embodied in LS-DYNA and KC-FEMFRE codes, or (2) RKPM meshfree method, as embodied in the KC-FEMFRE code. Two other formulations from LS-DYNA are briefly introduced for comparative purposes: these are the element-free Galerkin (EFG) and smooth particle hydrodynamics (SPH) formulations.

2. KC-FEMFRE features

The KC-FEMFRE code, which was based on an academic code developed during our previous work with UCLA (Chen and Crawford 2005, Crawford and Chen 2005, Chen and Crawford 2006, LS-DYNA 2007), provides a robust methodology and analysis capability for simulating the physics inherent in complex problems like those involving FPP/CDs using an approach that is based on first principals and avoids using ad hoc methods (e.g., erosion) and other methods lacking in rigor (e.g., hourglass control) that are now used to "fix" existing methodologies such as the Lagrangian finite element method so that they may be applied to such problems. Several examples of the effectiveness of the developed methods are given to demonstrate the capability of the new algorithms to solve penetration and impact types of problems and those involving intense blast loads (e.g., from contact charges).

The KC-FEMFRE code provides three different formulations for discretizing the domain of a problem, namely: LFEM, RKPM, and coupled LFEM/RKPM. A brief description of the features for these formulations is given below.

2.1. LFEM formulation

The LFEM formulation used by KC-FEMFRE is similar to that used by other LFEM codes (e.g., LS-DYNA) except for the way domain integration is performed. The LFEM formulation used by

KC-FEMFRE is based on nodal integration (Chen *et al.* 2002), whereas it is usually based on Gauss integration.

Since the finite element method is widely used for computing the responses of structural systems and components, there is a great body of experience as to its capability and manner of use related to a wide range of load types and response behaviors. More specifically, FEM codes like LS-DYNA are commonly used to compute responses produced by blast effects, and have been used extensively (e.g., Magallanes *et al*. 2008, Crawford and Morrill 2005, Crawford *et al.* 2001, Magallanes *et al.* 2009) to do so.

Moreover, the LFEM provides a robust and well-founded capability to perform complex physics-based analyses. Its advantages for solving FPP/CD problems include:

- Theoretically solid and well-developed over the past several decades.
- Wide availability of commercial software packages for its use.
- Applicability to many classes of complex engineering problems: solid mechanics, fracture mechanics, thermal mechanics, fluid-solid interactions, etc.
- The extensive experience gained with LFEM, its algorithms, coding, and accuracy of its results is invaluable in providing a guide to development of future analytic software.
- Computationally efficient and stable codes and algorithms.
- Provides a large library of material models and material modeling experience, which can be also used by the RKPM formulations.

These and other features have been instrumental in establishing the widespread use of LFEM codes in computing results for blast and impact effects problems.

However, the LFEM formulation has several major difficulties in addressing applications involving severe material distortions, preeminent of these are the difficulties encountered during calculations with excessive mesh distortion, the production of debris/ejecta, and fracturing, which commonly occur in FPP/CD analyses.

2.2. RKPM formulation

In contrast to LFEM formulations, the RKPM formulation offers the following advantages:

- Less restriction on the regularity requirement related to domain discretization.
- Direct nodal insertion/deletion capability (i.e., adaptive discretization).
- Smooth approximation for displacement, strain, and stress.
- Shape functions that are naturally conforming.
- Effective modeling of moving discontinuities.
- Suitable for multi-resolution analysis.
- Better convergence properties than LFEM.
- Affords an inherently simpler way to allow for the fracture and breakup of bodies and for simulating the effects of debris fields.

These advantages are crucial in solving the extreme blast and impact effects problems envisioned for the application of RKPM meshfree methods.

RKPM offers one other highly important advantage, especially as compared to other meshfree methods: its ability to use the same material models (i.e., both formulation and software) as those used by LFEM codes. This provides not only a great savings in theoretical and software development, but also means that the familiarity and success gained with LFEM material models and their code can be used to advantage by RKPM codes. This also makes evolutionary coupling of

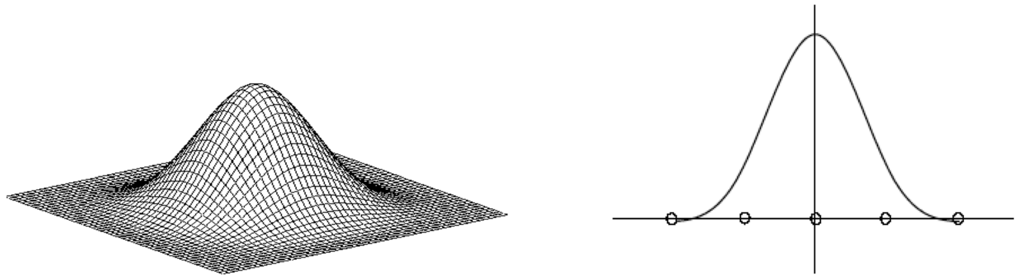

(a) RKPM shape function, shape function domain. (b) Section through a single shape function showing other particles covered by it.

Fig. 1 Depiction of RKPM shape function in two dimensions

LFEM and RKPM formulations much more straightforward than would otherwise be the case.

However, the RKPM formulation has several areas that need enhancement, whose address has been the focus of the KC-FEMFRE development work reported herein. These include:

- Complexity in implementing essential boundary conditions.
- Difficulties performing domain integrations.
- High CPU times required because of global shape function construction.
- Modeling material and body contact interfaces is more awkward with RKPM.

These issues are theoretically addressed in several references (Chen and Crawford 2005, LS-DYNA 2007, Chen *et al.* 1996, 1997, 1998, 2000, 2001, 2002, 2003, 2004, Chen and Wang 2000, 2005, You *et al.* 2002, 2003, Yoon and Chen 2002, Sze *et al.* 2004, Lu 2001, Wu *et al.* 2001, Yoon *et al.* 2001, Lu and Chen 2002, Chen and Wu 2006, Wang *et al.* 2003, Chen and Mehraeen 2004, 2005, 2006, Mehraeen and Chen 2004, Yoo *et al.* 2004, Wang and Chen 2004, Chen and Liu 2004). An RKPM shape function is shown in Fig. 1.

2.3. Coupled FEM/RKPM formulations

In many ways, RKPM and LFEM formulations are highly complementary of each other, especially in addressing each other's shortcomings-for example, the ability of RKPM to readily address LFEM mesh distortion and debris production problems, while LFEM is better able to handle issues related to boundary conditions, contact surfaces, and computational efficiency. This led to the notion that together they would offer a much better means to solve FPP/CD problems than either would separately.

Coupling these two basic analysis formulations (i.e., LFEM and RKPM) would seem to be the way to get the best of both worlds. But in the KC-FEMFRE code, this is taken one step further, and done in an evolutionary way such that, at the outset, the whole of the analytic model is characterized with the LFEM formulation. That is, only when the LFEM formulation breaks down (e.g., due to excessive mesh distortion) is it replaced with RKPM. Moreover, this is accomplished in a piecemeal fashion (i.e., FEM element by FEM element) and on the fly (i.e., in an evolutionary manner). In general, the solution process proceeds with a model, whose formulation is in flux, part RKPM and part LFEM, which regions of the model are covered by what formulation being in flux, as the action moves through the domain of the problem. This evolutionary process is part of each time step, and can work in both directions (i.e., from LFEM to RKPM and vice versa).

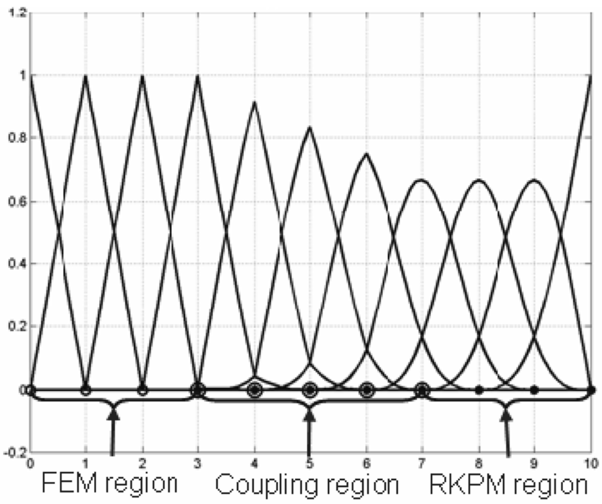

Fig. 2 Plot shows the blending of the shape functions for a coupled FEM and RKPM model

This capability is greatly aided by the use of the same material models for both formulations, but does require that the state variables employed by the LFEM (e.g., stress and strain) be computed and stored at nodal points (i.e., as compared to the conventional LFEM scheme of using the integration points). This latter requirement is readily accomplished by using a unified nodal integration for the whole problem domain (Chen and Crawford 2005, Crawford and Chen 2006).

An idealization of the coupling process is depicted in Fig. 2. Here the three zones inherent in a coupled model are shown, namely, the LFEM domain, the RKPM domain, and the transition zone between the two. Different ways of structuring the transition zone were evaluated in earlier studies (Chen and Crawford, 2005, 2006), which resulted in the selection of the form shown in Fig. 2, which is pretty much the simplest and most efficient and accurate form for doing this. The coupling of the RKPM and LFEM discretizations offers the following advantages:

- Higher computational efficiency (i.e., much shorter computational times) compared to use of only the RKPM method.
- Wider applicability compared to pure LFEM by modeling the difficult parts (i.e., those parts with high levels of material distortion) of the problem's domain with RKPM instead of an LFEM formulation.
- Straightforward application of essential boundary conditions by modeling most material and body boundaries with LFEM.
- Use of the same material models, which by-and-large can be taken directly from existing LFEM codes.
- Provides straightforward means to introduce adaptive discretization (e.g., increasing of the DOFs in a region of high strain gradients) into a model, which is much more easily done within the RKPM domain.

2.4. Evolutionary coupling of LFEM and RKPM discretizations

An effective means for performing evolutionary coupling of LFEM and RKPM was developed to allow the discretization of a model to be dynamically interchanged from LFEM to RKPM and vice versa in a piecemeal fashion with little loss of accuracy. The intent is to allow these two types of discretization to be interchanged as needed to address the complexities of the problem and minimize the CPU time. Evolutionary coupling is more demanding than the static coupling described in Section 2.3 because of the potential for accumulating errors as discretizations are interchanged during the solution process.

The primary objective of evolutionary coupling is to provide a more effective and accurate means to capture responses in highly distorted and damaged regions of the model. This would include regions involving the formation of shear band localization, damage propagation, crater and ejecta formation due to fragment impacts, and other complex behaviors related to weapon-target interactions. Having this capability will negate resorting to the heuristic rule-based procedures (e.g., erosion) that were used in the past with LFEM formulations to produce results for these behaviors.

An attractive modeling strategy that was implemented with evolutionary coupling in the KC-FEMFRE code involves initially using just an LFEM formulation to formulate the analysis model, so that at the outset of the calculation the responses are based only on a conventional LFEM approximation, which minimizes the CPU time and memory needed. If the complexity of the analysis is too great for the LFEM in a particular region, this region would evolve to an RKPM discretization. The method developed also supports the reverse operation (i.e., transforming an RKPM discretization into an FEM discretization).

2.4.1. Trigger criteria

One of the major features of the analytic modeling capability provided by KC-FEMFRE is the ability to start the analysis using an LFEM approach to model the whole domain of the problem. Then, based on some form of triggering device, the evolutionary coupling feature is invoked to allow the more robust RKPM approach to replace LFEM in regions where the complexities of the solution dictate that RKPM's more robust capabilities should be employed. This requires the development of a triggering criteria to initiate the process of replacing an LFEM region with an RKPM discretization and that would also indicate the extent of this transformation. The triggering process associated with evolutionary coupling is a separate task (i.e., from the coupling itself) and requires development of methodologies that can sense when a change is needed in the type of discretization.

Simplified versions of the triggering criteria are based on limit values placed on the state variables, deformations, and/or deformation gradients to define the extent and timing of the replacement of the LFEM discretization with an RKPM discretization. In the problems shown in the paper (Section 3), the damage index parameter provided by the K&C concrete model (Crawford and Malvar 2006) is used as the triggering criteria. This index indicates the level of damage experienced by the concrete. In summation, the intent is to replace regions of the LFEM discretization that are "in trouble" (e.g., due to excessive mesh distortion) with an RKPM discretization.

2.4.2. Unified domain integration for evolutionary FEM-RKPM coupling

To yield an effective evolutionary LFEM-RKPM coupling, accurate transfer of state and field variables from LFEM mesh to RKPM particles (nodes) is of critical importance. Initial attempts at evolutionary coupling of LFEM and RKPM discretizations had a fundamental problem of not smoothly transitioning from one domain to the other, which was caused in large part by the different locations used for calculating state variables; that is, at integration points for LFEM and nodal points for RKPM. This was resolved by using the same information scheme in both domains, namely, all the state variables are defined at the nodal points for both the LFEM and RKPM domains. This feature has allowed the smooth and robust coupling shown in the simulation problems presented.

To provide this common framework for calculation and storage of variables, a unified stabilized nodal integration technique was developed for both LFEM and RKPM so that all the state variables could be computed at the nodal points—note that the field variables already are calculated at a common location, namely, the nodal points. To achieve the needed uniformity for LFEM-RKPM coupling, an integration formulation was developed for LFEM using the same stabilized conforming and nonconforming nodal integration (SCNI and SNNI) methods that are used for RKPM, which are described in Section 2.5.

Having such a common system for the storage of state and field variables (i.e., the nodal points) provides an easy means to transfer them from LFEM nodes to RKPM nodes without performing interpolation. The effectiveness of using the SCNI method for integration in LFEM was shown in Choi *et al.* (2009).

2.5. Stabilized nodal integration

Domain integration is a key step in the RKPM formulation of the conservation equations (Wu 2005). Integration in the meshfree (RKPM) domain is not as simple as Gaussian and other quadratures used in domains where a mesh has been defined. To improve computational efficiency and avoid the use of an integration cell (i.e., mesh) for integration in RKPM, stabilized nodal integration methods were developed (Chen *et al.* 2001, 2002). Developing stabilization techniques for the integration process was a major milestone in creating a robust RKPM solution procedure free from the need of a background mesh to support the integration process. Fig. 3 shows the nodal representative domain Ω_L with boundary Γ_L for particle x_L created by a Voronoi diagram for the different forms of integration used by RKPM.

2.5.1. SCNI

To address the solution instabilities, several modifications to the nodal integration algorithms were made to ensure optimum convergence rates and stability. The resulting algorithm-labeled the Stabilized Conforming Nodal Integration (SCNI) (Chen *et al.* 2001, 2002)-produces much better results. This type of integration is depicted in Fig. 3(a) for particle x_L.

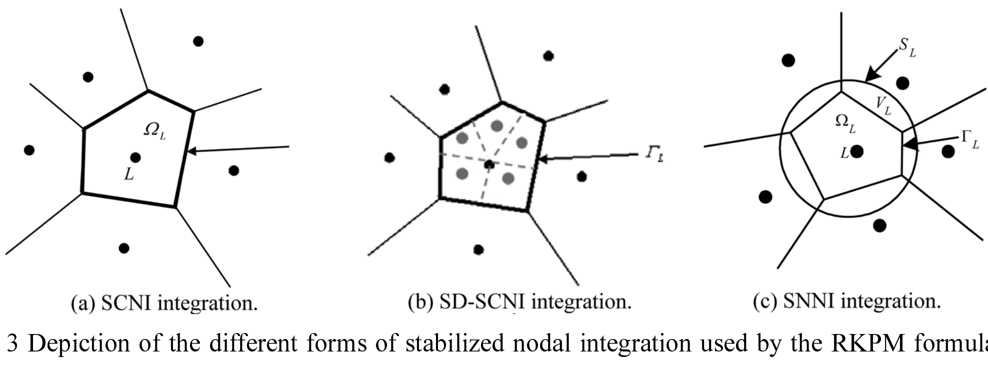

(a) SCNI integration. (b) SD-SCNI integration. (c) SNNI integration.

Fig. 3 Depiction of the different forms of stabilized nodal integration used by the RKPM formulation

2.5.2. SD-SCNI

However, the SCNI still exhibits stability problems for fast transient responses. The SCNI method was modified to produce an acceptable level of stability. This was accomplished by incorporating a subdomain integration scheme (Wu 2005).

This method is based on using the Voronoi cell, which provides a means to divide the RKPM domain into cells (i.e., small subdomains surrounding a particle). For the improved SD-SCNI method, the Voronoi cell is divided into a number of smaller cells (e.g., the five depicted in Fig. 3(b)). SD-SCNI is performed over the smaller cells to gain better stability and accuracy. This cell division is just for the purpose of integration and does not result in any changes in the shape functions themselves.

2.5.3. SNNI and SD-SNNI

For the semi-Lagrangian discretization (see Section 2.6), using SCNI is impractical for use in problems involving the modeling of large material distortions and material separations. For domain integration of the semi-Lagrangian RKPM formulation, a modified version of SCNI, called the SNNI (Chen and Wu 2006), was developed. SNNI stands for Stabilized Nonconforming Nodal Integration and is depicted in Fig. 3(c).

In contrast to SCNI where the strain smoothing is performed in the undeformed configuration, the strain smoothing for SNNI integration is computed in the deformed configuration. Moreover, SNNI is compatible with the strictures imposed by semi-Lagrangian RKPM and is computationally more efficient than SCNI for problems with large deformation and material distortions and material separations. In structural problems, the stability and accuracy of SNNI (Wu 2005) appears comparable to that of SCNI. In SNNI the strain smoothing is performed over a "non-conforming" smoothing domain V_L with boundary S_L, as shown in Fig. 3(c). With the smoothed strain computed in the smoothing domain V_L, the internal energy in the variational equation is integrated nodally. The SNNI method can be easily extended to large deformation problems, in which the deformation gradient is smoothed using the same approach.

In the RKPM formulation used in KC-FEMFRE, domain integration for problems with large distortions and high strain rates is performed using SNNI or a subdomain SNNI method (denoted SD-SNNI). Both methods were implemented under the framework of the semi-Lagrangian formulation; both methods may be used for the Lagrangian formulation as well.

2.6. Semi-lagrangian formulation

The Lagrangian formulation breaks down when the deformation gradient cannot provide a one-to-one mapping from the current configuration to the reference configuration, which typically occurs in extremely large deformation problems such as earth moving and projectile penetration. A semi-Lagrangian formulation was developed for this kind of extremely large deformation problem (Chen and Wu 2006, Wu 2005). The key difference between the Lagrangian and semi-Lagrangian formulations is the evaluation of kernel functions; this process is graphically illustrated in Fig. 4 (details are found in the references). The semi-Lagrangian approach is employed in analyses of penetrations problems in this work.

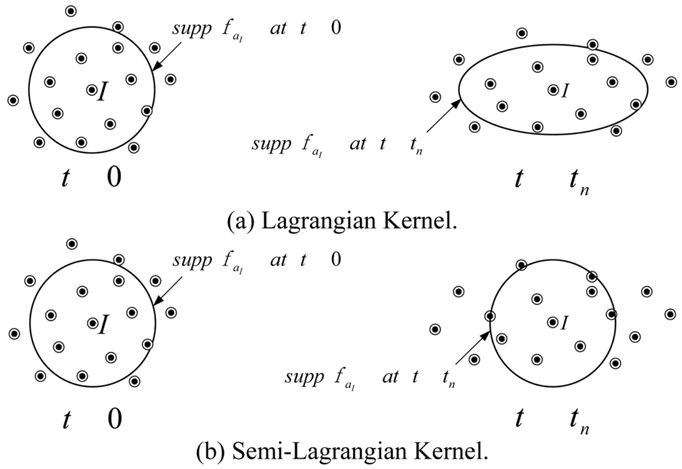

Fig. 4 Kernel support comparison of Lagrangian and semi-Lagrangian approaches; the dark circle encloses the domain of a particular shape function, that is, the one associated with I-th particle (or node)

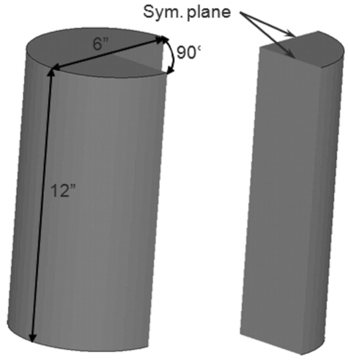

(a) Structure: an f_c' = 6,480 psi concrete cylinder.

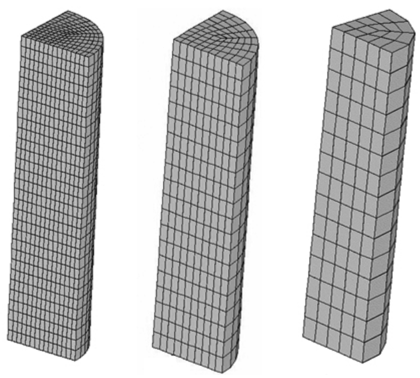

(b) Models used in analysis represents three different discretization. While a mesh is used in the graphic depicts the model, for the RKPM models it is used only to shown where the particles are located (i.e., at what would be the node point in an FEM model.

Fig. 5 Problem 1: compute behavior for UUC test: validation modeling

3. Benchmark problems for KC-FEMFRE

A series of benchmark problems were run to verify the basic capability offered by the KC-FEMFRE code and its RKPM formulation to capture key behaviors and behaviors of particular interest in solving FPP/CD problems. Some results for these problems are shown to demonstrate the basic capacity of the code.

Problem 1: Standard Concrete Cylinder Test. This problem involves the modeling of the standard unconfined uniaxial compression (UUC) test of a cylindrical concrete specimen. The model used is shown in Fig. 5. Results from this model of a UUC test and from models of similar types of tests are used to verify the performance of the K&C concrete material model, and its performance in the

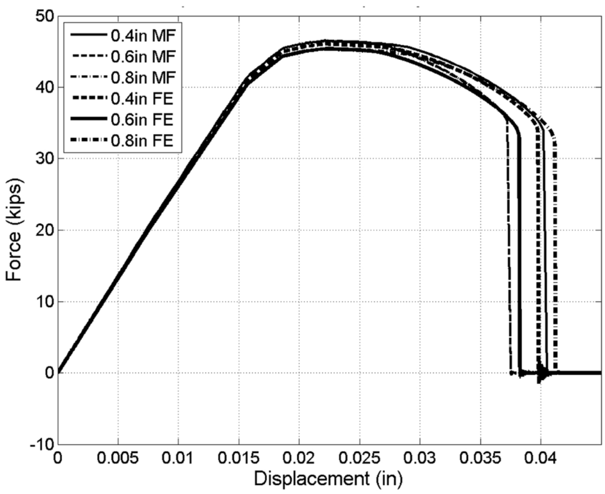

Fig. 6 Problem 1 results: indicating the effect of different formulations and discretizations.

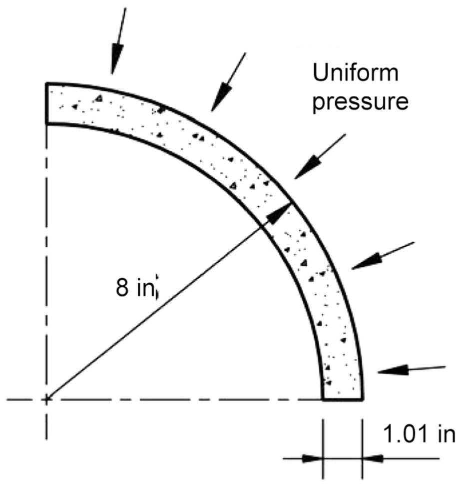

Fig. 7 Problem 2: implosion of a plain concrete cylinder; here the problem setup is shown; $f_c' = 6{,}180$ psi

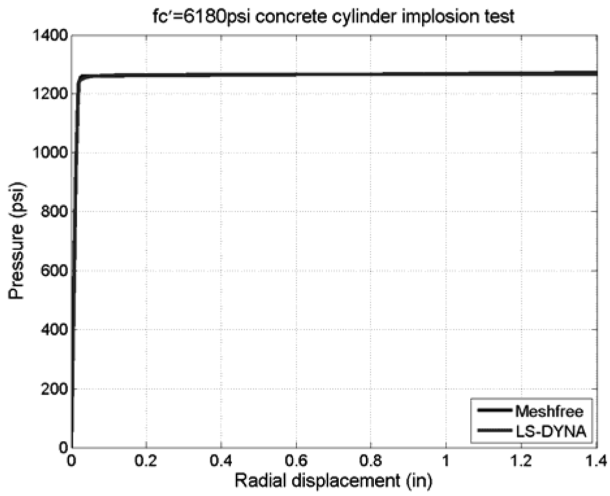

Fig. 8 Problem 2: results in terms of load-displacement; results from the two codes overlay each other

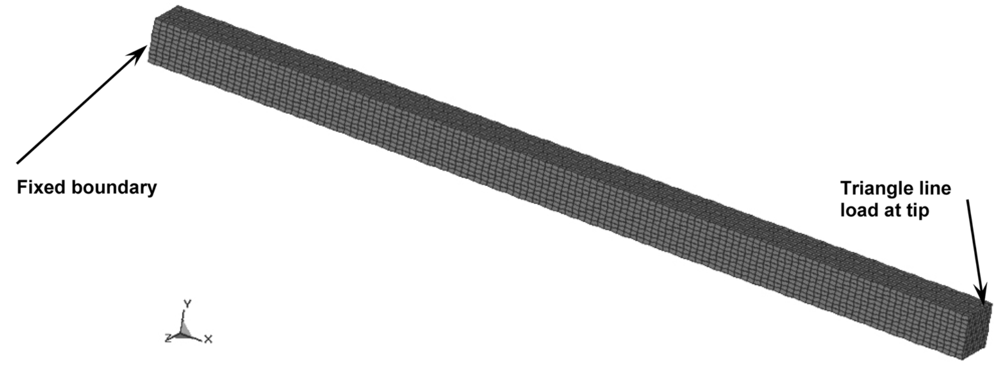

Fig. 9 Problem 3: model used to compute comparisons of cantilever beam responses

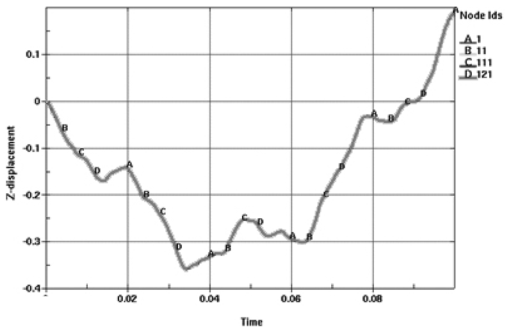

(a) FEM solids.

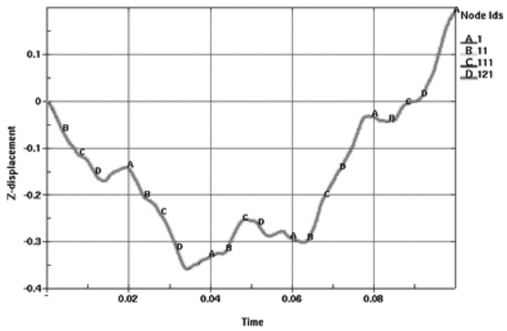

(b) EFG

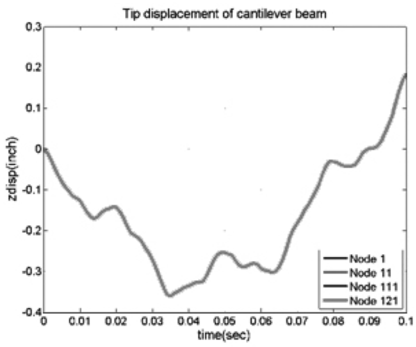

(c) RKPM

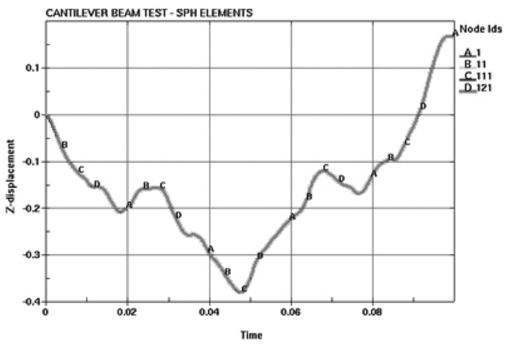

(d) SPH

Fig. 10 Problem 3A results: elastic deformations computed by different methods

KC-FEMFRE code. Results from both LS-DYNA and KC-FEMFRE are shown in Fig. 6 for the UUC test and three different discretizations.

Problem 2: Implosion of Concrete Cylinder. This problem involves a plain concrete cylinder (f_c' = 6,180 psi) that is subjected to an increasing hydrostatic pressure until it implodes. The problem setup is shown in Fig. 7. Results for this problem from KC-FEMFRE (using an RKPM discretization) and LS-DYNA (using an LFEM discretization) are presented in Fig. 8. Test data (Albertsen 1973) shows that implosion pressure for this cylinder is 1,420 psi: KC-FEMFRE and LS-DYNA produced identical results, predicting an implosion pressure of 1,260 psi.

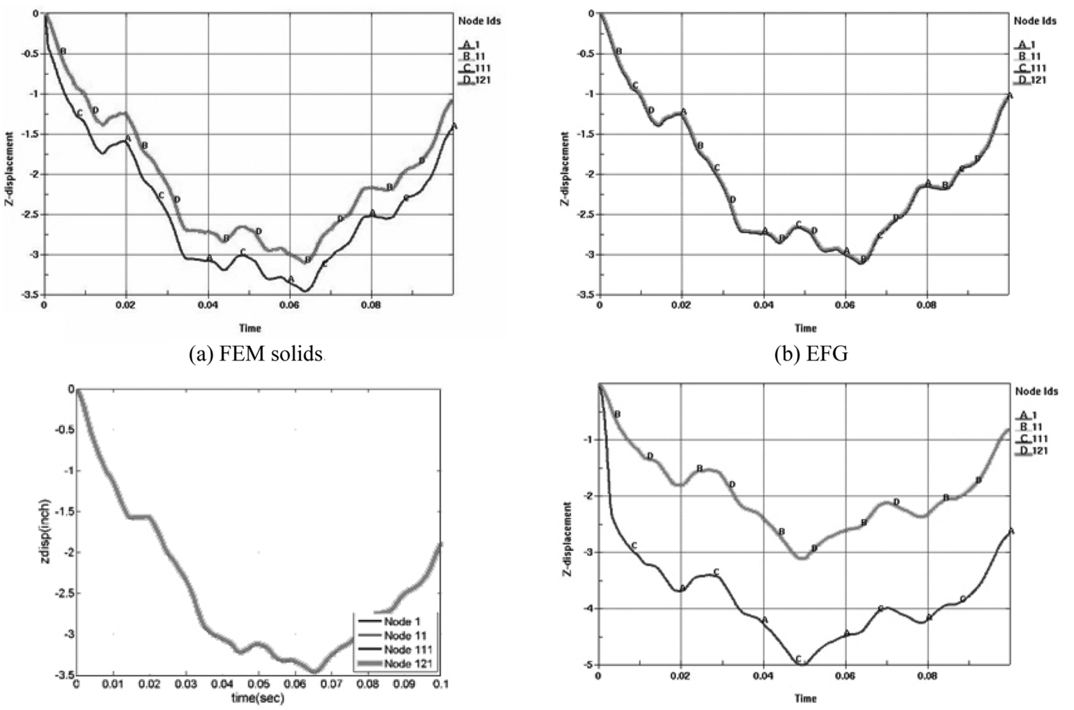

(a) FEM solids (b) EFG

(c) RKPM (d) SPH

Fig. 11 Problem 2B results: plastic deformations computed by different formulations

Table 2 Results summary and comparisons for Problem 3

Metric	Load p	Units	LFEM		EFG	SPH	RKPM
			Beam	Solids			
Peak tip displacement	500 psi	Inches	0.363	0.358	0.379	0.358	0.361
Plastic strain	500 psi	%	0	0	0	0	–
Peak tip displacement	4,000 psi	Inches	3.147	3.460	3.113	4.992	3.47
Plastic strain	4,000 psi	%	2.74	0.80	0.69	0.16	–
Time per step (μs)	–	–	6.3	3.7	3.7	11.3	2.5
CPU time	–	–	20 sec	30 min	4 h 30 m	1 h 2 m	1 h 26 m

Problem 3: Cantilever Beam. This problem involves computing the elastic and plastic responses of a cantilever beam (Fig. 9). Results are provided for four different formulations using the same von Mises material characterization: namely, RKPM, LFEM, EFG, and SPH. For the standard Lagrangian finite element method, two types of models are used: (1) using 8-node solid elements and single point integration with the discretization shown in Fig. 9 and (2) using beam elements with an analogous discretization. Two levels of loading, which is applied at the beam's tip, are applied: one causing an elastic response and another causing a plastic response. Results are summarized in Table 2 and shown in Figs. 10 and 11. As is shown, the LFEM results are computed in much less time than needed by the three MFM formulations shown (by about a factor of 3 in the case of RKPM).

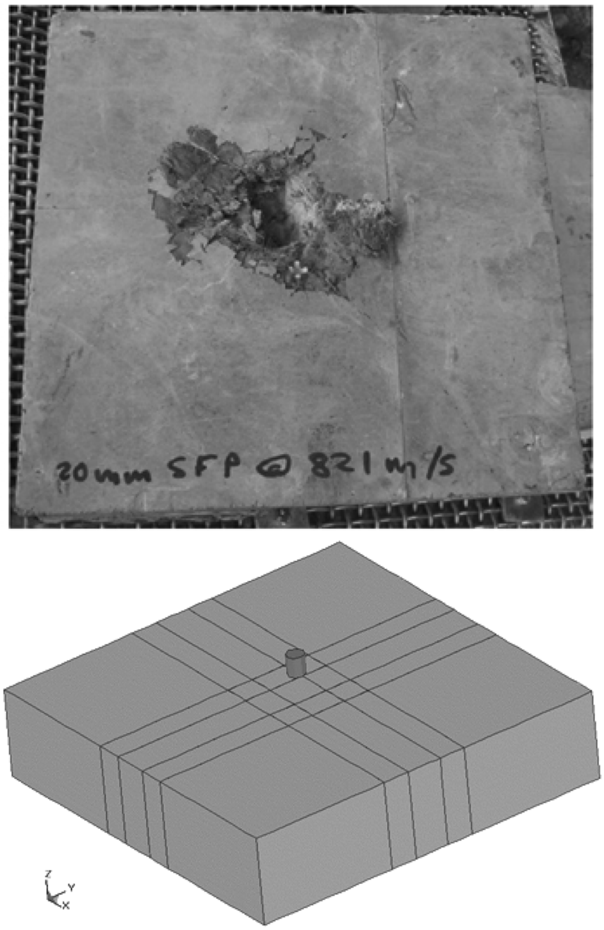

Fig. 12 Problem 4: calculation of damage caused by 20 mm FSP impact of a 100 mm UHPC panel at 820 m/s

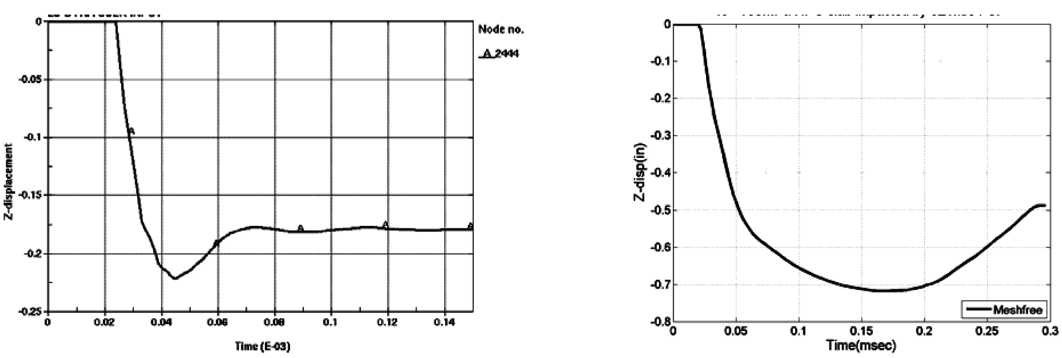

(a) LFEM (b) RKPM

Fig. 13 Problem 4: deformation history of the concrete surface at the point of impact

Problem 4: FSP Penetration Problem. This problem involves computing results for a test involving an FSP (i.e., fragment simulated projectile) striking a UHPC panel (i.e., constructed with ultra high-performance concrete). The setup and test results are shown in Fig. 12. Results for LFEM and RKPM models that are otherwise identical to each other were generated. Fig. 13 shows the penetration depths calculated by LS-DYNA and KC-FEMFRE using a semi-Lagrangian formulation. The test shows a penetration depth (i.e., depth of the impact crater) of 25 mm. LS-DYNA predicts a penetration depth of 5 mm, while KC-FEMFRE predicts a penetration depth of 19 mm.

4. Blast load problem

This problem (Problem 5) involves simulating the effect on a concrete slab of a near-contact charge with a coupled LFEM/RKPM model. The problem consists of a plain concrete slab (4×4×

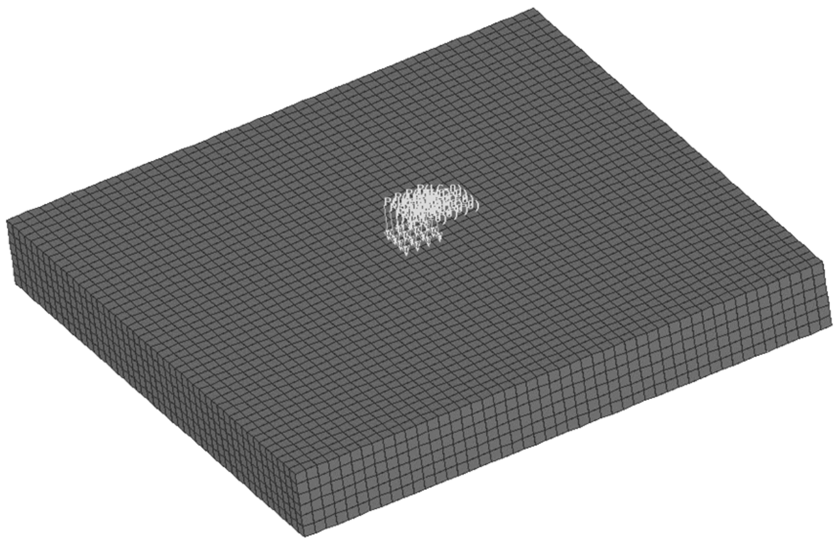

Fig. 14 Problem 5: concrete panel (f_c' =5,000 psi), triangular pulse (20 ksi by 3 ms)

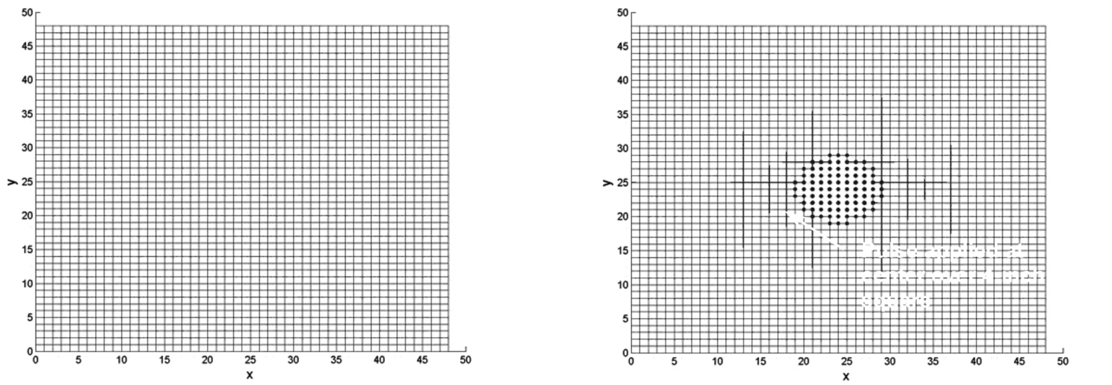

(a) At t = 0, the problem domain is covered by only an LFEM formulation

(b) At t = 250 μsec, a small RKPM region has replaced the LFEM formulation in the vicinity of the loading

Fig. 15 Problem 5 results: indicating the evolutionary nature of the coupling of RKPM and LFEM

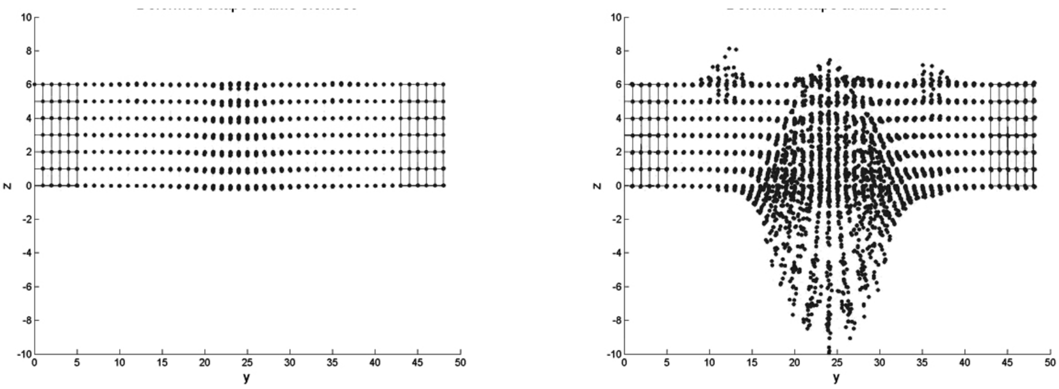

(a) t = 500 μsec. (b) t = 2,500 μsec.

Fig. 16 Problem 5 results: deformed shapes computed for mid plane section

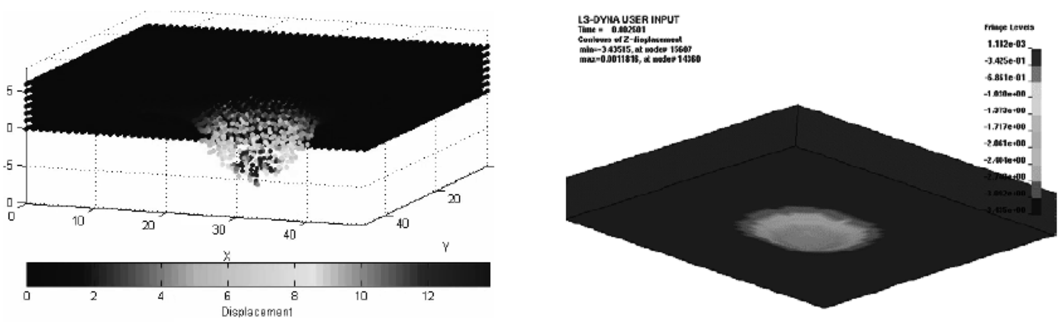

(a) RKPM (b) LFEM

Fig. 17 Problem 5 results: comparison of RKPM and LFEM (LS DYNA) at t=2,500 μsec

½-foot) subjected to an airblast having a triangular waveform with a peak pressure of 20 ksi and a duration of 3 ms (i.e., an impulse of 30 ksi-ms). The model for this problem is illustrated in Fig. 14.

In the analysis, the evolution from LFEM to RKPM is performed automatically. A specific value of the damage index that is computed by the K&C concrete model is used as the triggering mechanism that causes the transformation of an LFEM element to a set of RKPM nodes. Originally, the whole domain is modeled by LFEM, and then it evolves to RKPM as the triggering criterion is met. Some plots indicating the evolution of the transformations from LFEM to RKPM domains are shown in Fig. 15. The transformation can also be seen in the scatter plots on the yz-plane shown in Fig. 16 along with the deformations exhibited by the slab.

Comparisons of the deformations computed by KC-FEMFRE (using evolutionary coupling) and LS-DYNA (using LFEM) are shown in Fig. 17 at a time of 2,500 μs. These isometric views of the deformed slab indicate some significant differences in the response computed by the two formulations, where RKPM exhibits a decided amount of spallation while the LS-DYNA model does not. Fig. 18 shows comparisons of displacement and velocity histories between the KC-FEMFRE and LS-DYNA models for the top and bottom surfaces of the slab. In these plots, the velocity waveforms show a distinct difference for the two formulations.

5. Projectile impact problem

There exists a considerable amount of data pertaining to the effects resulting from the impacts on concrete targets of FSPs (fragment simulating projectiles). An example of one of these targets is shown in Fig. 19. The crater dimensions were the primary measurement extracted from the tests for use in these comparison studies. The geometry of the concrete target used for the comparative analyses performed herein is cylindrical with a radius and thickness of 12 inches. For the analyses reported herein, the 30.78 g FSP shot at 1,000 m/s was used for the tests and simulations.

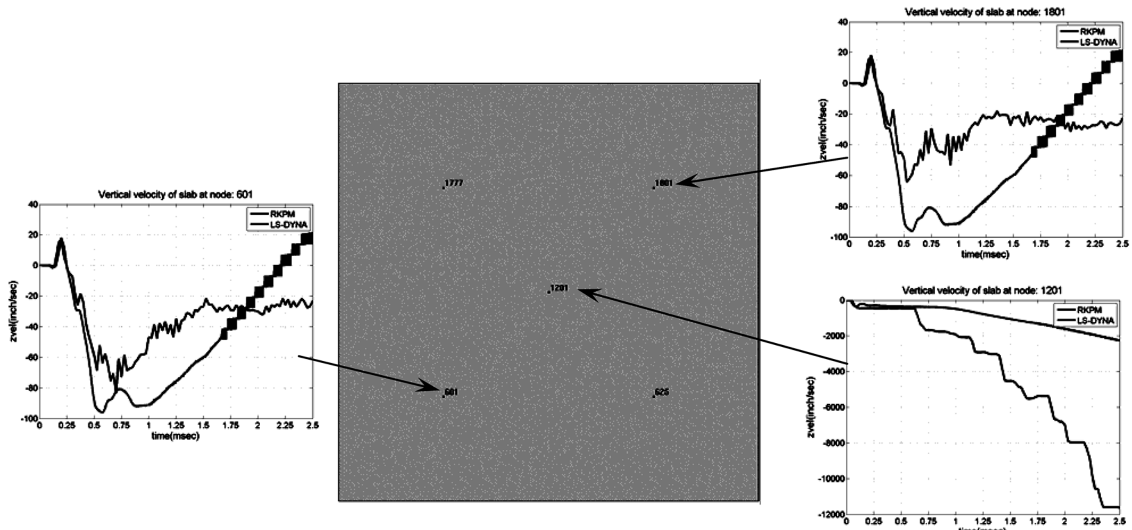

(a) Rear face

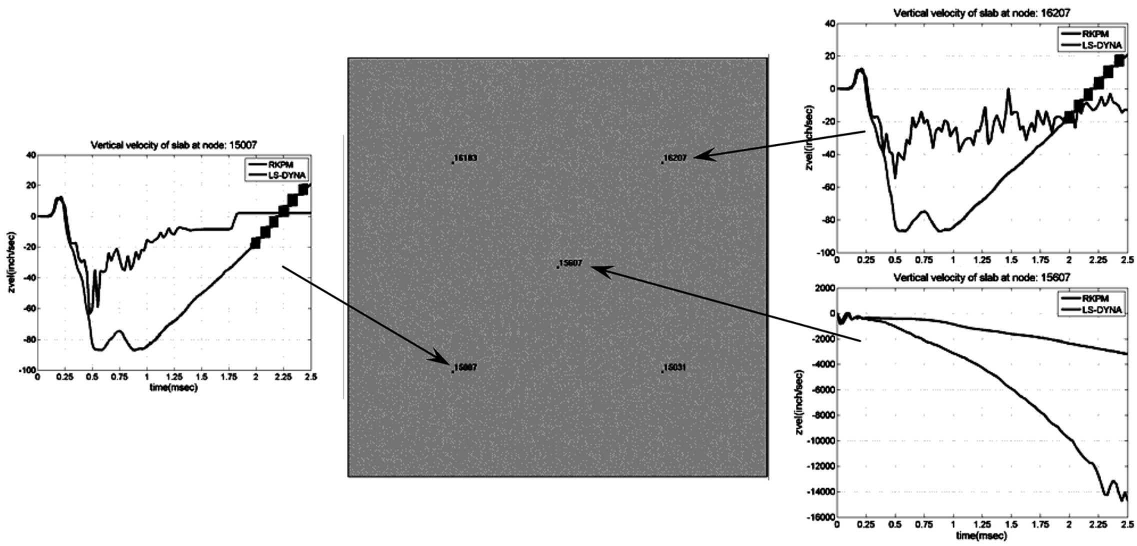

(b) Front face

Fig. 18 Problem 5 results: comparison of velocity histories computed using RKPM and LFEM (LS DYNA) models

Table 3 Effect of artificial viscosity on LFEM results for Problem 6

Case	Discretization		Hourglass Control, QM[1]		Energy[3] Ratio, %	Crater Depth, inches		Comments
	Size inches	Type	IHQ[2]	QM		Apparent[4]	Actual[5]	
1.1		LFEM	3	0.14	10	1.21	1.45	
1.2	¼	LFEM	3		26	1.12	1.35	
1.3	½	LFEM	3		43.5	0.81	1.17	
1.4	1	LFEM	3		49.2	0.48	0.74	
1.5	2	LFEM	3		32.3	0.21	N/A	
2.1	½	RKPM	N/A	N/A	0	1.05	1.93	
2.2	¼	RKPM	N/A	N/A	0	0.99	1.83	
3.1[4]	½	LFEM	3	0.14	45.2	0.90	1.64	Default values
3.2	½	LFEM	3	0.04	33.1	1.30	1.61	Little self penetration
3.3	½	LFEM	5	0.01	11.8	1.50	1.98	
3.4	½	LFEM	5	0.01	13.7	1.65	2.19	

[1]Hourglass control type specification in LS-Dyna (3:Flanagan-Belyschko viscous form with exact volume integration for solid element, 5: Flanagan-Belyschko stiffness form with exact volume integration for solid element)
[2]Hourglass coefficient
[3]Ratio of the hourglass energy to the total energy.
[4]Computed depth of crater is taken from the deformation of the node on the target's surface directly beneath the point of impact.
[5]The actual crater depth is gotten by removal of the highly damage material from the crater, as indicated by the K&C concrete model's damage parameter (i.e., material with a damage above 95%).
[6]f_c'=25 MPa for Cases 3.1, 3.2, 3.3, and 3.4.

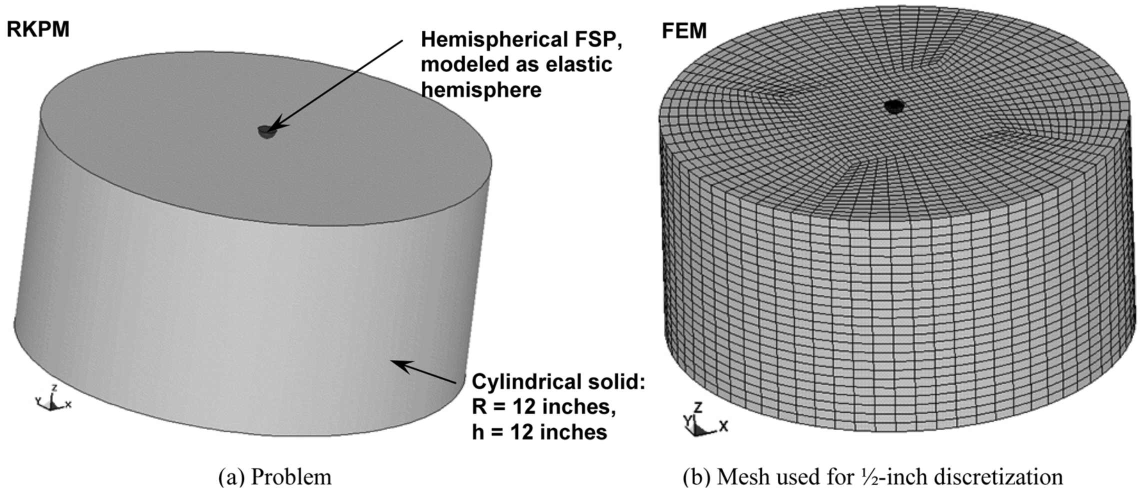

(a) Problem (b) Mesh used for ½-inch discretization

Fig. 19 Problem 6: example of HFPB model used in calculating penetration of concrete target by an FSP

Convergence studies using two different analytic formulations (i.e., LFEM and RKPM) were performed to determine effective and practical levels of discretization for each in performing analyses of fragment impacts. The influence on the results from fragment impact simulations of different discretizations and kinds of analytic formulations was examined by comparative studies of data generated from a suite of analyses. In these calculations, the K&C concrete (KCC) model (Crawford and Malvar 2006) was used to characterize the target structure using material parameters representative of a generic 35 MPa (5,000 psi) concrete, which was assumed as the target's material.

The primary objective in performing these convergence and effects studies is to obtain a comparison of each of these codes in their capacity to predict the penetration depth measured in the test. A second objective is to identify the effect of resolution on the penetration depth computed, the damaged area, and the transferred momentum. In addition, it is important to gauge the error, at least qualitatively, that results with the coarser models (i.e., discretizations larger than ½-inch), since this level of discretization in modeling is more in keeping with those that would be used in actual structural response calculations. Information such as this is important because each of the factors studied can affect an RC member's response when subjected to the hundreds of primary fragment impacts that might ensue from a cased explosive.

Cases Run. Results for Problem P6 were generated using different ways to construct the analytic models of the target and characterize the FSP. The intent being to identify the key parameters and modeling features needed for this type of problem and what level of influence might be associated with specific parameter types and values. Results are shown for:

- Different ways to compute crater depth
- Different levels of discretization.
- Different formulations to solve the problem (i.e., LFEM and RKPM methods)
- The effect of using different levels of artificial viscosity for the LFEM model.

The cases run are summarized in Table 3.

5.1. Determining crater depth

Determining crater depth is not as straightforward in the analysis as it might appear. Two methods were studied:

- Method 1, determining apparent crater depth: here, the depth of crater is taken from the deformation of the node on the component's surface directly opposite the point of impact.
- Method 2, determining actual crater depth: here, the crater depth is gotten by removal of the highly damage material from the crater. This material is identified by the value of the damage

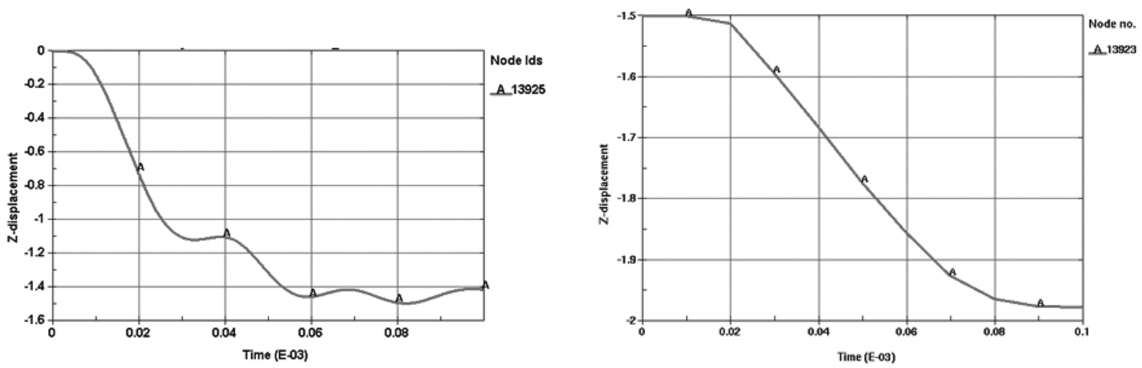

(a) Apparent crater

(b) Actual crater depth (based on removal of material with 95% damage)

Fig. 20 Problem 6 (case 3.3, LFEM, IHQ=5, QM=0.01): comparison of apparent and actual crater depths

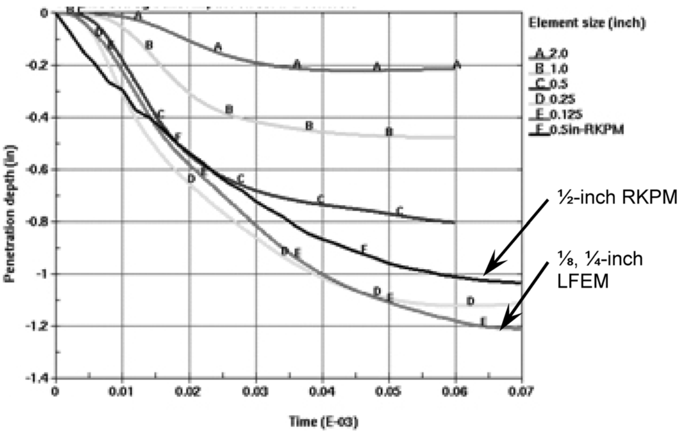

Fig. 21 Problem 6: effects on apparent crater depth predictions of the level discretization; LFEM results for meshes ranging from 2-inch elements to 1/8-inch elements; RKPM results shown for ½-inch discretization

parameter computed by the K&C concrete model (i.e., material with a damage above 95% is removed).

Crater depth results based on using these two methods are given in Table 3. The results shown in Table 3 indicate that the depth of the actual crater may be 20-30% larger than that of the apparent crater. Plots of crater depth evolution with time for both the apparent and actual crater depths for one case are presented in Fig. 20.

5.2. Effect of discretization

Results showing the influence of different levels of discretization, ranging from 2-inch to 1/8-inch mesh resolutions, are shown in Fig. 21. Most of these results are from LFEM models, while one is for a ½-inch RKPM discretization. The comparison of LFEM results shown in Fig. 21 demonstrates that the level of discretization has a significant impact on the results for this problem, unless a mesh size of less than ¼-inch is used for the LFEM model. In fact, results seem to be unaffected by the discretization for only discretizations of less than ¼ inch for LFEM and around a ½-inch for RKPM. This may present a serious problem in some analyses since this level of discretization is likely to be impractical for many analysis problems.

5.3. Effects of hourglass control parameters

In LS-DYNA, the effects of the hourglass control and contact algorithm parameters may have an untoward influence on the response. To ensure that the LS-DYNA responses were not unduly influenced by these parameters, a study of these effects on Problem P6 results was performed. In general, we would want the hourglass parameters to be set so that the hourglass energy is as low as possible consistent with the requirement of preventing excessive hourglassing and element entanglement. Table 3 shows the influence of these parameters on the calculation of the apparent crater depth for the ½-inch LFEM discretization.

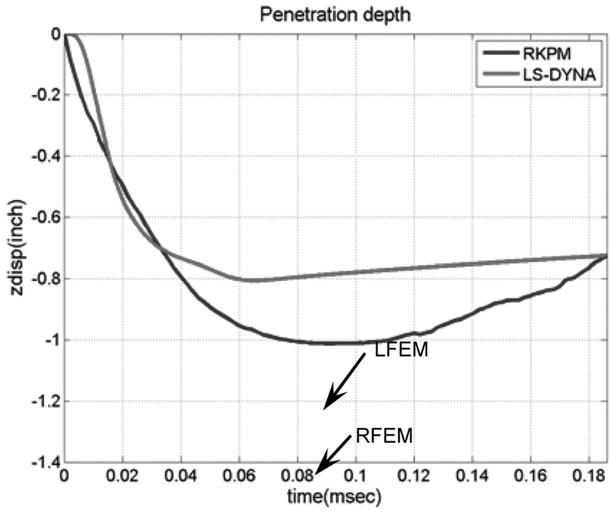

Fig. 22 Problem 6: comparison of apparent crater depth computed using two different analysis formulations (i.e., LFEM and RKPM)

5.4. Effect of analytic formulation

To assess whether a different formulation would influence the computed crater depth, results from LS-DYNA (i.e., from the LFEM formulation) were compared to results for the identical problem that were computed by KC-FEMFRE (i.e., from an RKPM formulation). Results from the KC-FEMFRE code are shown in Fig. 21. For these results, the ½-inch discretization was used.

Fig. 22 shows a direct comparison of the apparent crater depth histories computed by LFEM and RKPM methods for a ½-inch discretization. KC-FEMFRE predicts 20% more deformation than the equivalent LS-DYNA simulation. The RKPM results provide some reassurance as to the validity of both RKPM and the LFEM results since the RKPM methodology does not suffer from the common numerical issues encountered by LFEM for penetration problems related to mesh tangling, hourglass modes, and artificial viscosity. These issues may be contributors to the differences shown between the KC-FEMFRE and LS-DYNA results, but are probably not the main reasons.

6. Conclusions

KC-FEMFRE performed well in the benchmark and verification problems presented, either matching traditionally generated results or performing better. The benchmark problems that do not involve extreme loadings (i.e., Problems 1 to 3) demonstrate that RKPM (KC-FEMFRE) and LFEM (LS-DYNA) produce quite similar results. In contrast, for the extreme loadings represented by Problems 4 and 5, there are substantial differences in the predictions. In the results computed for Problem 6 (Table 3), influence of nodal density, hourglass parameters (only used for the LFEM models), and formulation were evaluated. For the LFEM formulation, the hourglass control specified is quite influential on the apparent depth calculated, producing values ranging from 0.9 inch for the default viscosity to 1.65 inches, as shown in the table. Such a variation provides demonstrative evidence of a key advantage afforded by RKPM that of not having to use such an ad hoc device as hourglass control.

Several important new features were incorporated into the KC-FEMFRE code that had not been addressed in the previous MFM codes, namely evolutionary coupling, subdomain integration, and the K&C concrete model. Other features of the code are listed in Table 1. These features were instrumental to producing the capability shown by KC-FEMFRE for the above applications. Results for the benchmark run (Choi *et al*. 2009, Chen and Crawford 2005, 2006, Crawford and Chen 2005), some of which were shown herein, indicate that the code is performing properly and is quite robust in its ability to solve problems with large amounts of material distortions and rapid load rates.

The theoretical basis for the code's development, by and large, can be found in earlier K&C/UCLA work (Choi *et al.* 2009, Chen and Crawford 2005, 2006, Crawford and Chen 2005). Of particular importance to the applications shown for "extreme loading" problems are several recent theoretical improvements:

- Enhanced essential and natural boundary condition enforcement. In the current KC-FEMFRE code, arbitrary time dependent concentrated force, surface traction such as blast load, and prescribed displacement can be enforced.
- Expansion of material library. The K&C concrete model and piecewise linear plasticity model are now available in the KC-FEMFRE code.
- Improved stability on domain integration. A 3-dimensional subdomain integration was developed, which allowed a stable solution to be obtained for high-velocity impact problems using a semi-Lagrangian formulation.
- Evolutionarily-coupled FEM/RKPM simulation. Predefined semi-automated and a fully-automated coupling is provided by the code.

The KC-FEMFRE code was shown to provide a versatile platform from which to assess the unique capabilities provide by the RKPM methodology and by the evolutionary coupling of the LFEM/RKPM formulations.

References

Albertsen, N.D. (1973), "Influence of compressive strength and wall thickness on behavior of concrete cylindrical hulls under hydrostatic loading", Technical Report, R 790, Naval Civil Engineering Laboratory, Port Hueneme, CA, June.

Chen, J.S. and Crawford, J.E. (2005), "Development of meshfree methods for fragment impact problems", *Karagozian Case,* Burbank, CA, TR-04-38.3, July.

Chen, J.S. and Crawford, J.E. (2005), "Theoretical development of meshfree methods for fragment impact, penetrations, and other weapon-target interaction problems", *Karagozian Case,* Burbank, CA, TR-05-40.1, September.

Chen, J.S. and Crawford, J.E. (2006), "Development of 3-Dimensional meshfree methods for fragment impact problems", *Karagozian Case,* Burbank, CA, TR-06-57.1, December.

Chen, J.S., Han, W., You, Y. and Meng, X. (2003), "A reproducing kernel method with nodal interpolation property", *Int. J. Numer. Meth. Eng.*, **56**, 935-960.

Chen, J.S., Kotta, V., Lu, H., Wang, D., Moldovan, D. and Wolf, D. (2004), "A variational formulation and a double-grid method for meso-scale modeling of stressed grain growth in polycrystalline materials", *Comput. Method. Appl. M.,* **193**, 1277-1303.

Chen, J.S. and Liu, W.K. (2004), "Meshfree methods: recent advances and new applications", *Comput. Method.*

Appl. M., **193**, 3-6.
Chen, J.S. and Mehraeen, S. (2004), “Variationally consistent multiscale modeling and homogenization of stressed grain growth”, *Comput. Method. Appl. M.*, **193**, 1825-1848.
Chen, J.S. and Mehraeen, S. (2005), “Multi-scale modeling of heterogeneous materials with fixed and evolving microstructures”, *Model. Simul. Mater. Sc.*, **13**, 95-121.
Chen, J.S. and Mehraeen, S. (2006), “Wavelet galerkin method in multiscale homogenization of heterogeneous materials”, *Int. J. Numer. Meth. Eng.*, **66**(3), 381-403.
Chen, J.S., Pan, C. and Wu, C.T. (1997), “Large deformation analysis of rubber based on a reproducing kernel particle method”, *Comp. Mech.*, **19**, 211-227.
Chen, J.S., Pan, C., Roque, C.M.O.L. and Wang, H.P. (1998), “A lagrangian reproducing kernel particle method for metal forming analysis”, *Comp. Mech.,* **22**, 289-307.
Chen, J.S., Pan, C., Wu, C.T. and Liu, W.K. (1996), “Reproducing kernel particle methods for large deformation analysis of nonlinear structures”, *Comput. Method. Appl. M.*, **139**, 195-229.
Chen, J.S., Roque, C.M.O.L., Pan, C. and Button, S.T. (1998), “Analysis of metal forming process based on meshless method”, *J. Mater. Process Tech.,* **80-81**, 642-646.
Chen, J.S. and Wang, D. (2005), “Extended meshfree method for elastic and inelastic media”, *Lect. Notes Computat. Sci. Eng.*, **43**, 17-38.
Chen, J.S., Wang D.D. and Dong, S.B. (2004), “An extended meshfree method for boundary value problems”, *Comput. Method. Appl. M*., **193**, 1085-1103.
Chen, J.S. and Wang, H.P. (2000), “New boundary condition treatments for meshless computation of contact problems”, *Comput. Method. Appl. M.,* **187**, 441-468.
Chen, J.S., Wu, C.T. and Belytschko, T. (2000), “Regularization of material instabilities by meshfree approximation with intrinsic length scales”, *Int. J. Numer. Meth. Eng.*, **47**, 1303-1322.
Chen, J.S., Wu, C.T., Yoon, S. and You, Y. (2001), “A stabilized conforming nodal integration for galerkin meshfree methods”, *Int. J. Numer. Meth. Eng.*, **50**, 435-466.
Chen, J.S., Wu, C.T., Yoon, S. and You, Y. (2002), “Nonlinear version of stabilized conforming nodal integration for galerkin meshfree methods”, *Int. J. Numer. Meth. Eng.*, **53**, 2587-2615.
Chen, J.S. and Wu, Y. (2006), “Stability in lagrangian and semi-lagrangian reproducing kernel formulation using nodal integration in nonlinear solid mechanics”, *Computat. Method. Appl. Sci*., **5**, 55-76.
Chen, J.S., Zhang, X. and Belytschko, T. (2004), “An implicit gradient model by a reproducing kernel strain regularization in strain localization problems”, *Comput. Method. Appl. M.*, **193**, 2827-2844.
Choi, H.J., Wu, Y. and Crawford, J.E. (2009), “Description of the coupled FEM/RKPM analysis code and its theoretical basis”, *Karagozian Case,* Burbank, CA, TR-09-16.1, June.
Crawford, J.E. and Chen, J.S. (2005), “Description of meshfree methods developed for fragment impact, penetrations, and other weapon-target interaction problems”, *Karagozian Case,* Burbank, CA, TR-05-47.2, September.
Crawford, J.E., Hasselman, T., Bogosian, D.D., Anderson, M. and Dunn, B. (2001) “Development of fast running response models for air-backed reinforced concrete walls for the MEA code”, *Karagozian Case,* Burbank, CA, TR-01-05.1, August.
Crawford, J.E. and Malvar, L.J. (2006), “User's and theoretical manual for k&c concrete model”, *Karagozian Case,* Burbank, CA, TR-06-19.1, March.
Crawford, J.E. and Morrill, K.B. (2005), “Evaluation of methods for protecting reinforced concrete columns from satchel charges”, *Karagozian Case,* Burbank, CA, TR-05-9.1, August.
Dancygier, A.N. (2009), “Characteristics of high performance reinforced concrete barriers that resist non-deforming projectile impact”, *Struct. Eng. Mech.* **32**(5), 685-699.
LS-DYNA Keyword User’s Manual - Version 971,” Livermore Software Technology Corporation, May 2007.
Lu, H. (2001), “Progressive adaptivity formulation in galerkin meshfree method”, Ph.D. Thesis (Advisor: J.S. Chen), University of Iowa.
Lu, H. and Chen, J.S. (2002), “Adaptive meshfree particle method”, *Lect. Notes Computat. Sci. Eng.*, **26**, 251-267.
Magallanes, J.J., Crawford, J.E. and Morill, K.B. (2008), “Overview of the development of fast-running physics-based models for: analysis of steel column/Girder, AF05-167; predicting the response of brick and stud walls, AF05-152; response of concrete block masonry walls, AF03-143”, *Karagozian Case,* Burbank, CA, TR-08-30.1,

September.
Magallanes, J.M., Fu, S. and Morrill, K.B. (2009), "Fast-running models (FRMs) for concrete masonry unit (CMU) walls subjected to munitions effects - Phase II Final Report, Volume 1", *Karagozian Case,* Burbank, CA, TR-07-8.2, March.
Magallanes, J.M., Lan, S., Wu, Y. and Morrill, K.B. (2009), "High-fidelity physics-based (HFPB) analysis of cmu walls subjected to blast load", *Karagozian Case,* Burbank, CA, TR-09-18.1, June.
Mehraeen, S. and Chen, J.S. (2004), "Multiscale wavelet-based homogenization of heterogeneous media", *Finite Elem. Anal. Des.*, **40**, 1665-1679.
Sze, K.Y., Chen, J.S., Sheng, N. and Liu, X.H. (2004), "Stabilized conforming nodal integration: exactness and variational justification", *Finite Elem. Anal. Des.,* **41**, 147-171.
Teng, T.L., Shih, T.M. and Lu, C.C. (2008), "Effect of design parameters on the anti-penetrating properties of space armor", *Struct. Eng. Mech.* **28**(6), 715-725.
Wang, D. and Chen, J.S. (2004), "Locking free stabilized conforming nodal integration for meshfree mindlin-reissner plate formulation", *Comput. Method. Appl. M.,* **193**, 1065-1083.
Wang, D., Chen, J.S. and Sun, L. (2003), "Homogenization of magnetostrictive particle-filled elastomers using an interface-enriched reproducing kernel particle method", *Finite Elem. Anal. Des.*, **39**, 765-782.
Wu, C.T., Chen, J.S., Chi, L.C. and Huck, F. (2001), "A lagrangian meshfree formulation for geotechnical materials", *J. Eng. Mech.,* **127**, 440-449.
Wu, Y. (2005), "A Stabilized semi-lagrangian galerkin meshfree formulation for extremely large deformation analysis", Ph.D. thesis, UCLA.
Yoo, J.W., Moran, B. and Chen, J.S. (2004), "Stabilized conforming nodal integration in the natural-element method", *Int. J. Numer. Meth. Eng.*, **60**, 861-890.
Yoon, S. and Chen, J.S. (2002), "Accelerated meshfree method for metal forming simulation", *Finite Elem. Anal. Des.,* **38**, 937-948,
Yoon, S., Wu, C.T., Wang, H.P. and Chen, J.S. (2001), "Efficient meshfree formulation for metal forming simulation", *J. Eng. Mater. Tech. - ASME*, **123**, 462-467.
You, Y., Chen, J.S. and Lu, H. (2003), "Filters, reproducing kernels, and adaptive meshfree methods", *Comput. Mech.*, **31**, 316-327.
You, Y., Chen, J.S. and Voth, T. (2002), "Characteristics of semi- and full discretizations of stabilized galerkin meshfree method", *J. Finite Elem. Anal. Des.*, **38**, 999-1012.